Improved core transport triggered by off-axis ECRH switch-off on the HL-2A tokamak

Z. B. Shi, Y. Liu, H. J. Sun, Y. B. Dong, X. T. Ding, A. P. Sun, Y. G. Li, Z. W. Xia, W. Li, W.W. Xiao, Y. Zhou, J. Zhou, J. Rao, Z. T. Liu, Q. W. Yang, X. R. Duan

Southwestern Institute of Physics, P. O. Box 432, Chengdu 610041, China

Corresponding Authors's e-mail address: shizb@swip.ac.cn

Abstract: The reduced core transport and the internal transport barrier (ITB) are observed after the ECRH is turned off in the HL-2A tokamak plasmas. It is found that the time delay of the central temperature afer ECRH switch-off increases as the ECRH deposition moves from center to edge. After the far off-axis ECRH switch-off (outside q=2 surface), the central temperature transiently increases for several tens of milliseconds before it starts to drop. A low-frequency, spectrally broad, poloidal structure that peaks near zero frequency is observed in the core region (near q=1 surface) by using the newly developed correlation reflectometer system. These structures have low poloidal mode number, high polodal correlation and short radial correlation comparable to the ambient turbulence decorrelation length. Observation shows that these structures play an important role in the suppression of the core turbulence, and in the improvements of the core transport after the off-axis ECRH is turned off.

1. Introduction

Anomalous transport is one of the most important topics in fusion plasmas as it degrades the overall confinement. Many experiments have been performed on various devices to clarify the formation of the transport barrier with reduced transport triggered by localized heating and fuelling, such as pellet injection, supersonic molecular beam injection (SMBI), high Z impurity injection and electron cyclotron resonance heating (ECRH) [1-7]. There are two types of explanations relating to these phenomena [5-7]. One is relevant to the current profile, the magnetic shear or plasma rotation. The other one is relevant to the so-called non-local effects, whose theories have not been well developed so far. In the off-axis ECRH experiments, observations in T-10 and TEXTOR suggest that the necessary condition to reduce the core transport after ECRH switch-off is relevant to the appearance of the low value of dq/dρ near rational q-surfaces [4, 5]. A large increase on the central electron temperature is induced by off-axis ECRH in DIII-D, which was modeled in terms of a significant heat pinch and the suppression of the heat diffusivity [3]. However, previous off-axis ECRH experiments in several devices was mostly carried out around r/a~0.4 [4-6]. The core turbulence study is not sufficient. It is still unclear about the links between the improved confinement, the ECRH power deposition and the core turbulence.

In this work, experiments with various ECRH depositions (from r/a=0 to 0.7) by changing the toroidal magnetic field have been carried out on the HL-2A tokamak (major radius R = 1.65m, minor radius a = 0.4m) [8]. Significant results are as follows: The delayed drop of the central temperature after ECRH switch-off depends on the ECRH deposition

position. In the case of far off-axis (outside q = 2 surface) ECRH switch-off, the central electron temperature significantly increases for several tens of milliseconds before it starts to drop, while the edge electron temperature immediately decreases. This relates in time with the significantly suppression of the central turbulence and the enhancement of the low frequency poloidal structures. These structures play an important role in the suppression of the core turbulence, and in the improvements of core transport after the off-axis ECRH heating is turned off.

The remained parts in this paper are arranged as follows. Section 2 contains a description of the experimental arrangement. The reflectometer systems for the density profile and turbulence measurements are presented. The statistics of delayed drop of the central temperature after ECRH switch-off are described in section 3. The turbulence and the correlation of the low frequency fluctuations are explained in section 4. The summary is given in section 5.

2. Experimental arrangement

To measure the long range correlation, such as MHD and zonal flow, a reflectometer system for the density correlation measurement has been developped in this work. Figure 1 shows the schematic view of the microwave reflectometers on the HL-2A tokamak. Four O-mode reflectometers with the horizontal launching and receiving antena array are installed. One reflectometer with the frequency of 20 GHz (cutoff density: $0.5*10^{19}$ m^{-3}) is arranged in the horizontal plane. The other three reflectometers with the frequency of 35 GHz (cutoff density: $1.5*10^{19}$ m^{-3}) are arranged in the poloidal and toroidal directions. The microwave Gunn sources with the output power up to 200 mW are used to improve the signal to noise ratio. The launcing and receiving antenna array are installed in the vaccum. The Teflon is used as the electric isolator and airproof between the tokamak and the reflectometer system. The poloidal and the toroidal intervals of the 35 GHz reflectometers are about 32 cm, which corresponds to the poloidal and toroidal angles of 0.8 rad and 0.2 rad, respectively. Therefore, the spatial resoultions are much longer than the turbulence decorrelation length. Nevertheless, it is engouh to measure the long range correlation, such as low m MHD and zonal flow. The beam waist is about 6 cm at 20 cm away from the launching antenna. By ray tracing simulation [9], we found that the receiving signal is a hybrid between microwave reflectometry and scattering, which is sensitive to the density fluctuation.

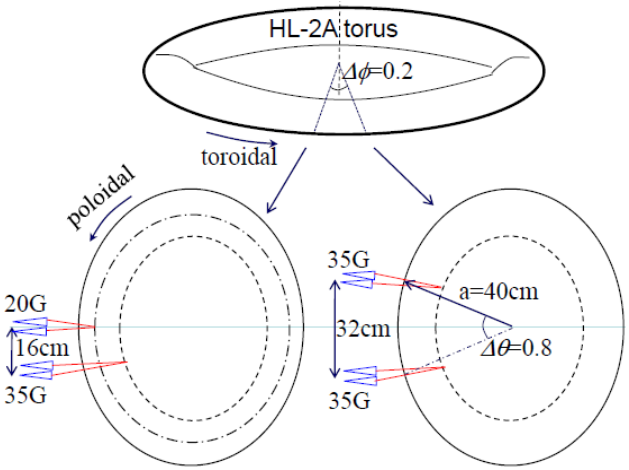

Fig. 1. Schematic view of the microwave reflectometers for the density correlation measurement.

The density profiles are measured by the 8 HCN interometers and an AM reflectomer (26-40GHz, (0.8-2.0)*10^{19} m^{-3}). The details of the measurements are given in references [10, 11], respectively. The electron temperature is measured by the 16-channel microwave heterodyne radiometer, which has a 73GHz/110GHz local oscillator. In this work, 73GHz microwave source is used as the local oscillator in the case of B_t ~1.3Tesla. Signals of 16-channels are obtained simultaneously with the frequency range covering from 74.5GHz to 97GHz with an interval of 1.5GHz. The electron temperature profile is calibrated by two-temperature method and the electron temperature is absolutely calibrated by Thompson scattering [12].

The turbulence is meaured by the correlation reflectometer system in the ECRH discharges. The ECRH system on HL-2A consists of six gyrotrons [13]. Six gyrotrons can operate together with the development of PSM power supplies for cathode. The obtained output power of each is up to 500 kW with a duration of 1s and a frequency of 68 GHz. In this work, the ECRH power is scanned from 300 kW to 1500 kW. The deposit position of ECRH is determined by the toroidal magnetic field. A toroidal field B_t = 1.22 Tesla is set for on-axis heating, while B_t = 1.3-1.4 Tesla is for off-axis heating. The toroidal field is scanned from 1.25 Tesla to 1.45 Tesla shot by shot to adjust the ECRH deposition position. The plasma current is about I_p = 160-180 kA. The line averged density is about (1-1.5)*10^{19} m^{-3}. It is estimated that the reflections are at radii r/a = 0.0-0.5 for the 35 GHz reflectometers and r/a = 0.5-1.0 for the 20 GHz reflectometer, respectively.

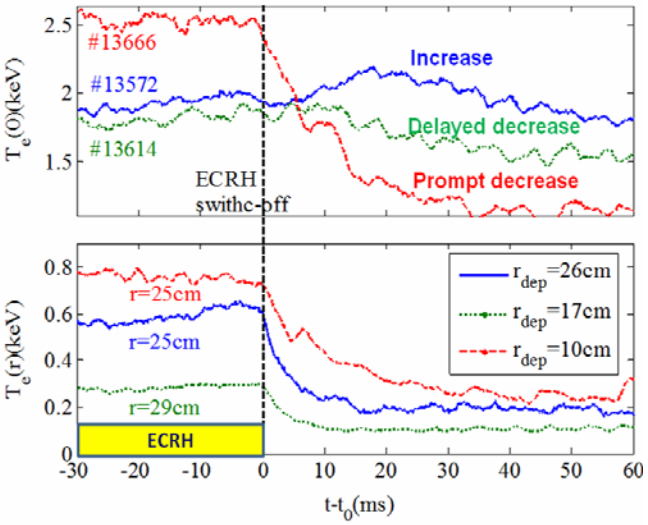

Fig. 2. Time evolutions of the (a) core and (b) edge temperatures after ECRH switch-off. The delayed decrease of the core temperature is observed after far off-axis ECRH switch-off.

3 Statisticis of ECRH switch-off experiments

Experiments with various ECRH deposition positions by changing the toroidal magnetic field have been carried out. Figure 2 shows time evolutions of the core and the edge temperatures after the ECRH is turned off. Three typical discharges with different ECRH deposition positions are

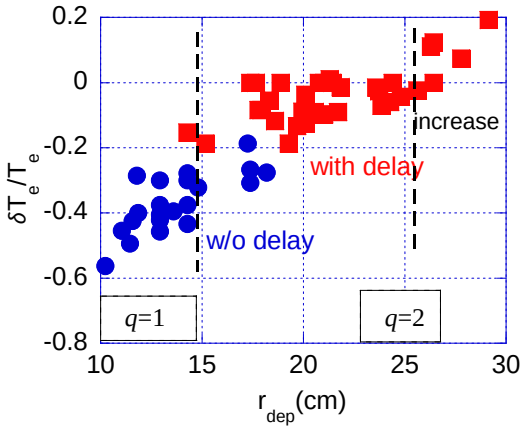

Fig. 3. Statistics of $\delta T_e(0)/T_e(0)$ as a function of ECRH deposition by changing the toroidal field.

plotted. In the case of on-axis ECRH, the core and the edge temperatures have simultaneous responses to the ECRH switch-off. They start to drop almost at the same time. As the ECRH deposition position moves from center to edge, the delayed drop of the central temperature is observed. When the ECRH deposition position is at the plasma edge (far off-axis ECRH, outside q = 2 surface), the increased central temperature after ECRH switch-off is observed. The edge temperature always exhibits simultaneously drop immediately after the ECRH is turned off. The central temperature increases for several tens of milliseconds before it starts to drop. This corresponds to the formation of an internal transport barrier (ITB) in the plasma.

Figure 3 shows statistics of $\delta T_e(0)/T_e(0)$ as a function of ECRH deposition position by adjusting the toroidal magnetic field in the ECRH discharges. The discrepancy of the central temperature is obtained 20 ms after the ECRH is turned off. The filled squares and dots denote with and without delay of the core temperature after the ECRH is turned off, respectively. The estimated ranges of q = 1 and q = 2 surfaces are plotted by dashed lines. We found that there are three domains related to the delayed drop of the central temperature. In the case of on-axise ECRH (inside q = 1 surface) switch-off, the central and the edge temperatures exhibit simultaneously drop. A delayed drop of the central temperature is observed if the ECRH deposition is between q = 1.0-2.0, which is similar to the observations in T-10 and TEXTOR tokamaks [5]. The delayed drop of the central temperature becomes strong when the ECRH deposition position moves from center to edge. In thes case of far off-axise ECRH (outside q = 2 surface), an increase of the central temperature is observed. This suggests that the core transport is significantly suppressed and the transport barrier is enhanced.

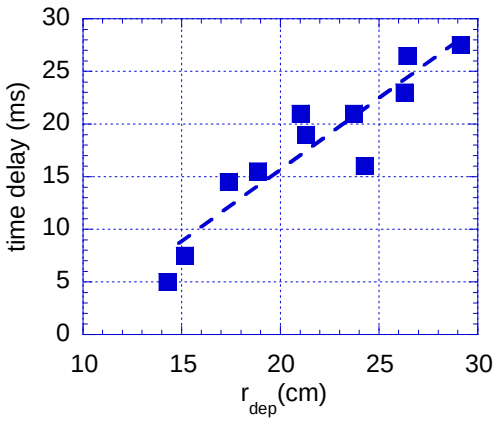

Fig. 4. Time delay of the central temperature drop v.s ECRH deposition.

The time delay of the central temperature drop after ECRH switch-off depends on the ECRH deposition position. Figure 4 shows the ECRH deposition dependence on the time delay of the central temperature after the ECRH is turned off. The time delay is about 10 ms when the deposition is at r = 16 cm (r/a = 0.4). It is about 25 ms if the ECRH deposition is at r = 27 cm (r/a = 0.68). The time delay is linearly increased as the ECRH deposition moves from center to edge. So the delayed drop of the central temperature becomes significant after the far off-axis ECRH switch-off.

4 Turbulence and transport

In this paper we will concentrate on the results with far off-axis (near q = 2 surface) ECRH switch-off, where the effect is most pronounced. Figure 5 shows (a) time evolutions of the electron temperatures and (b) temperature profiles in a typical far off-axis ECRH discharge (#13593). The ECRH with the power of 740 kW is deposited at r = 27.8 cm (r_{dep}/a ~0.69).

The q = 1 surface obtained from inverted sawtooth is at r = 12 cm. The whole electron temperature increases during ECRH heating. There are two domains relating to the evolutions of the electron temperatures after the ECRH is turned off, which are indicated by the dashed lines shown in Fig. 5(a). In the first domain (I) the central temperature is rapidly increased with the suppression of the sawtooth fluctuations. The edge temperature is rapidly decayed to equilibrium state. In the second domain (II), the central temperature starts to drop when the edge temperature drops to the equilibrium state. The sawtooth activities are gradually enhanced when the central temperature starts to decay. The increment of the central electron temperature is observed inside the q = 1 surface. This corresponds to the formation of an internal transport barrier near q = 1 surface.

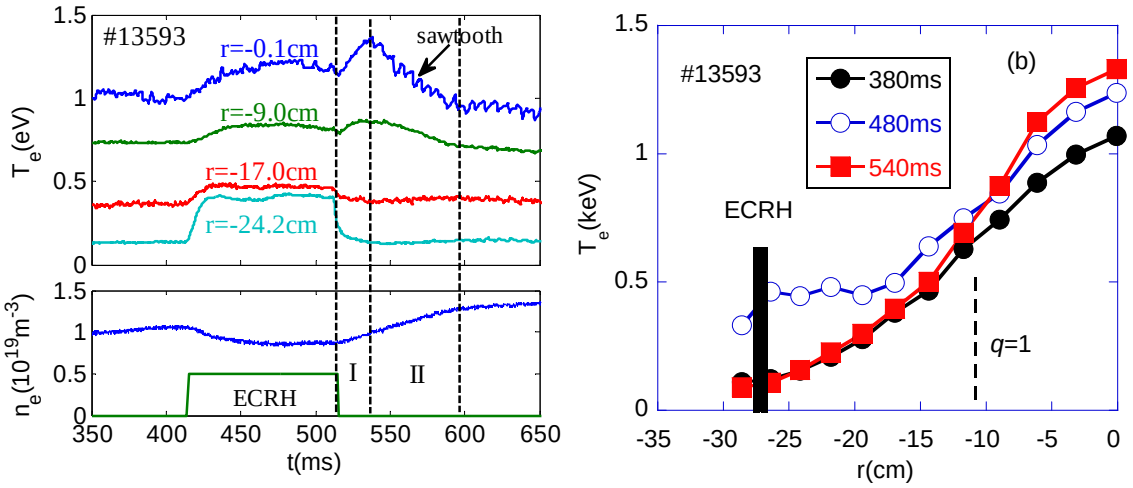

Fig. 5. (a) Time evolution of the electron temperature and density after ECRH switch-off (at 515 ms) (shot#13593, B_t=1.42 T, I_p=170 kA, P_{ECRH}=740 kW). The ECRH resonance is at 27.8cm (r_{dep}/a ~ 0.69); (b) Temperature profiles at 380 ms, 480 ms and 540 m;

The density fluctuations are measured by the O-mode correlation reflectometers. Figure 6 shows the power spectra of the density fluctuations measured by 35GHz reflectometer before (380 ms), during (480 ms) and 25 ms after (540 ms) ECRH. Their temperature profiles are shown in Fig. 5. The cutoff surface is estimated at r/a = 0.1-0.5 in this shot since the line averaged density is about (1-1.4)*10^{19} m^{-3}. Before ECRH, the m/n = 1/1 mode with the frequency of 3 kHz is observed. The power spectrum after ECRH switch-off is much lower than that before or during ECRH. This suggests that the central turbulence is suppressed after the ECRH is turned off. It is interesting to find that the low frequency fluctuation (f < 2 kHz) is increased and it is higher than that before ECRH. Note that the low frequency

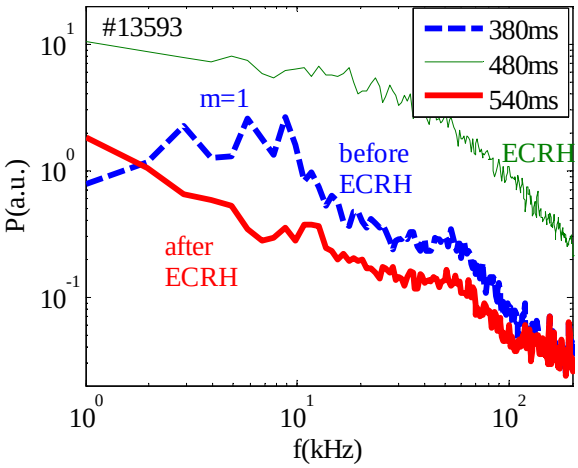

Fig. 6. power spectrum showing the turbulence suppression after ECRH switch-off. The ECRH power deposited at 27.8cm (r_{dep}/a ~0.69)

fluctuation is not the m = 1 mode, because the frequency of m = 1 mode is about 3kHz and it is transiently suppressed after ECRH is turned off.

To further understand this phenomenon, a shot (#14251) with the parameters similar to that shown in Fig. 5 is analyzed. The ECRH with the power of 611 kW is deposited at about r = 26 cm (r/a = 0.65). The central turbulence is measured by 35 GHz reflectometer. Its power spectra and cutoff radius are shown in Fig. 7. The ECRH is switched off at 575 ms. Since the electron density gradually increases after ECRH, the cutoff of 35GHz moves from r_c/a = 0.1 to 0.5. One can find that the high frequency fluctuation (f > 5 kHz) is significantly reduced, and the low frequency mode (f < 5 kHz) is enhanced after ECRH switch-off. This suggests that the low frequency mode and the high frequency turbulence are coupled through nonlinear transition. Suppression of the high frequency turbulence may enhance the low frequency mode.

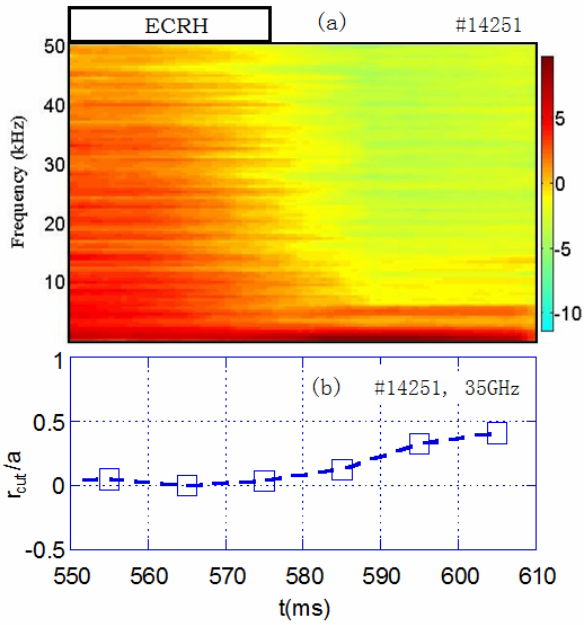

Fig. 7. (a) Power spectra and (b) cutoff radius of the central turbulence measured by 35GHz reflectometer in shot#14251 with B_t=1.41T, I_p=170kA and P_{ECRH}=611kW. The ECRH resonance is at about 26cm (r/a=0.65). The turbulence is significantly reduced after ECRH.

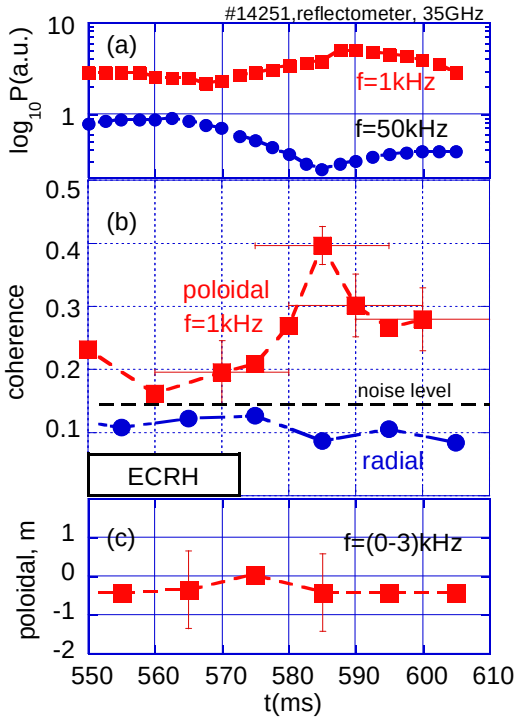

Fig. 8. Time evolutions of (a) the density fluctuation amplitudes (1kHz, 50kHz), (b) the poloidal and radial coherencies, and (c) the poloidal mode number.

Figure 8 shows time evolutions of (a) the density fluctuation amplitudes (1 kHz and 50 kHz) and (b, c) their cross correlations. The poloidal cross correlation is analyzed by using the signals measured by 35 GHz reflectometers. The fifty FFT windows with the time scale of 1 ms each and the ensemble average technique are used for the power spectrum within 10 ms. The details of the data analysis can be found in many literatures [14]. After ECRH is turned off, the fluctuation amplitude of 1 kHz starts to increase while that of 50 kHz starts to decrease. The poloidal coherence of the low frequency (1kHz) mode gradually increases. For

the high frequency fluctuation, the coherence is lower than the noise level. The radial coherence is obtained from 20 GHz and 35 GHz reflectometers. Although the radial coherence is lower than the noise level due to large radial interval (>10cm), a slight decrease is observed after ECRH is turned off. This may corresponds to the decrease of the radial correlation. The low frequency fluctuation has a low poloidal mode number (m = 0-1). The maximum coherence is observed at r_c/a ~ 0.2 (near the q = 1 surface). The transient increase of the poloidal coherence suggests that these low m modes are poloidal elongated near the q=1 surface.

The electron heat diffusivity is measured by the heat pulse propagation method and the transport properties are obtained in the confinement region outside the q = 1 surface. This method has been used to calculate the electron heat diffusivity in the typical L-mode plasma in HL-2A tokamak [15]. The electron heat diffusivity is given as

$$\chi_e = (r^2 - r_{mix}^2)/8t_p \qquad (1)$$

where r_{mix} is the mixing radius, and t_p is the heat pulse transfer time.

Figure 9 shows the electron heat diffusivity measured by sawtooth heat pulse propagation during ECRH, 15ms and 60ms after ECRH. The heat diffusivity is about 5 m^2s^{-1} 60 ms after ECRH. Since the central temperature already decays to equilibrium state, it can be considered as the heat diffusivity in ohmic plasma. After ECRH switch-off, the heat diffusivity decreases to 3.5 m^2/s, which is only half of that in ECRH. Therefore, the transport is transiently reduced by a factor of two. Figure 10 shows time evolutions of the confinement time and the poloidal magnetic fluctuation (5-200 kHz). The confinement time is increased by a factor of three because of the slightly increase of the electron density after ECRH. This is in agreement with the suppressions of the magnetic fluctuation and the core turbulence.

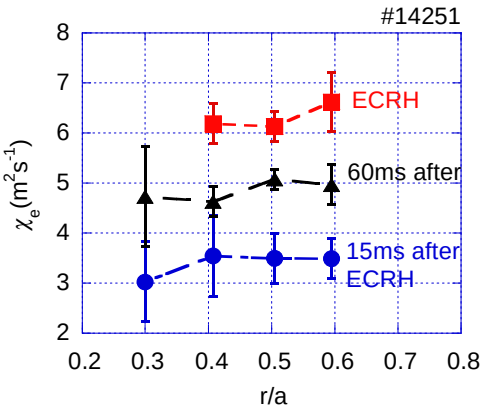

Fig. 9. The heat diffusivity measured by sawtooth heat pulse propagation

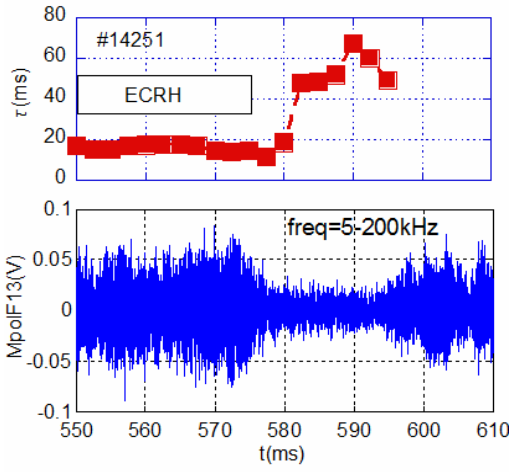

Fig. 10. Time evolutions of (a) confinement time and (b) poloidal magnetic fluctuation (f=5-100kHz)

5 Summary

Experiments for the core transport investigation have been carried out in HL-2A with various

ECRH deposition positions by changing the toroidal magnetic field. The statistic analysis of the changes of the central temperature after ECRH switch-off show that the time delay of the central temperature after ECRH switch-off increases as the ECRH deposition position moves from center to edge. After far off-axis ECRH (deposited outside the $q = 2$ surface) switch-off, the central temperature transiently increases several tens of milliseconds before it starts to drop. An internal transport barrier is observed near the $q = 1$ surface. The core turbulence is significantly suppressed, and the transport is transiently decreased by a factor of two after ECRH switch-off. This is relevant to the observed low frequency poloidal structures deeper into the core region of the plasma (near $q = 1$ surface). These poloidal elongated structures play an important role in the formation of the thermal barrier near $q = 1$ surface and in the reduction of the core turbulence and transport. Nevertheless, the formations of these structures are still unknown. Although there are several plausible mechanisms relating to the observed phenomena, such as the central low frequency zonal flow, non-local transport, the plasma rotation or the magnetic shear [5-7,16-18], present observations are not sufficient. Further works such as their 3D structures, rotation profiles and the central magnetic shear are necessary to confirm the observed low frequency modes.

Acknowledgements
The authors would like to thank Professor K. Nagasaki in Kyoto Univ. for the helps on ECE diagnostics. This work is supported by the National Natural Science Foundation of China under Grant No 11005037.

References:
[1] McKee G., et al., Phys. Rev. Lett. (2000)1922
[2] Connor J. W., et al. 2004, Nucl. Fusion, 44, R1.
[3] Callen J. D. et al. 1997, Plasma Phys. Control. Fusion, 39, B173
[4] Hogeweij G. M. D., et al. 1998, Nucl. Fusion, 38, 1881.
[5] Razumova K. A., et al. 2004, Nucl. Fusion, 44, 1067.
[6] Dong Y. B., et al., 22rd IAEA FEC, 2008, EX/P3-8
[7] Sun H. J., et al., 2010, Plasma Phys. Control. Fusion, 52, 045003
[8] Liu, Y., et al., Nucl. Fusion 45 (2005) S239.
[9] Lin Y., et al., Plasma Phys. Control. Fusion, 43(2001) L1
[10] Zhou Y., et al., Plasma Science and Technology, 11(2009) 413
[11] Xiao W. W., eta al, Plasma Science and Technology, 8(2006) 133
[12] Xu D. M., et al., Nucl. Fusion Plasma Phys. **20** (2000) 38 (in Chinese)
[13] Duan, X. R., et al., Nucl. Fusion 49 (2009) 104012.
[14] Shi Z. B., et al., Plasma and Fusion Res. 3 (2008), S1045
[15] Shi Z. B., et al., Plasma Science and Technology, 9(2007),534 .
[16] Qu W X *et al* 2000 *Nucl. Fusion Plasma Phys.* **20** 129 (in Chinese)
[17] Fujisawa, A., et al., Nucl. Fusion **49 (**2009) 013001.
[18] Zhao, K.J., et al., 23rd IAEA FEC, Daejeon, Korea, 2010, EXC/7-3.